2022

Design of a Direct-Contact Thermal Energy Storage Heat Exchanger for the NIST Net-Zero Residential Test Facility: Part 1 Flow Observation

Mark A. Kedzierski

Lingnan Lin

Design of a Direct-Contact Thermal Energy Storage Heat Exchanger for the NIST Net-Zero Residential Test Facility: Part 1 Flow Observation

Mark KEDZIERSKI*, Lingnan LIN

National Institute of Standards and Technology,
Gaithersburg, Maryland, USA
301-975-5282, mak@nist.gov

* Corresponding Author

ABSTRACT

This paper describes the first part of the design of a direct-contact heat exchanger (DCHEX) to be used for thermal energy storage in the Net-Zero Energy Residential Test Facility (NZERTF) at the National Institute of Standards and Technology (NIST). The heat exchanger was designed for heat exchange between a phase-change material (PCM) and refrigerant. The design required the selection of a PCM that would be immiscible with the refrigerant and have a freezing point temperature of approximately 285 K. A key facet of the present investigation was the construction of a test apparatus to observe the flow between the refrigerant and the freezing PCM to ensure a well-distributed flow and one where the refrigerant could flow past the frozen PCM. The companion paper, Part 2, presents a design for direct-contact heat exchange between the PCM octanoic acid and the refrigerant R410A.

1. INTRODUCTION

Test experience with the NIST Net-Zero Energy Residential Test Facility (NZERTF), Fanney et al. (2015), shows that the air-source heat pump (ASHP) consumes approximately 40 % - the largest share - of the home's total energy (Payne, 2018). Reducing its energy consumption is difficult because the Coefficient of Performance (COP) of conventional ASHPs is close to the theoretical thermodynamic limit. The COP decreases as the difference between the indoor and outdoor temperatures (i.e., the "lift" against which the ASHP works) increases (ASHRAE, 2015). The lift is directly related to the space conditioning need, therefore the heat pump will operate at a lower efficiency during the time when the building thermal load is greatest and higher efficiency when the demand is low. An analysis of the NZERTF data showed that operating the heat pump during times of the day with more favorable lift can increase the heating COP from 2.3 to 4.6 and the cooling COP from 4.3 to 5.5 (Payne, 2018). Consequently, a non-conventional ASHP that mitigates the characteristic of decreased efficiency at increased load is one approach to exceed the current state-of-the-art performance. In addition, reduced electricity needs for cooling during peak energy times and increased use at night is highly valued by the utilities.

A proposed solution for improved energy management that incorporates Thermal Energy Storage (TES) with a Phase Change Material (PCM) into a residential air conditioner was modeled by Kedzierski et al. (2018). They showed that a non-conventional ASHP with improved efficiency during electrical peaks used 6 % to 33 % less energy than the conventional system. Some of this improvement is because the PCM provided all of the cooling needs during the peak times when air conditioning operational efficiency is low, and some improvement is due to the fact that the unit runs nearly continuously instead of cycling on and off to meet the load, thus, avoiding a typical 2 % to 8 % loss in efficiency due to cycling (Baxter and Moyers 1985). When the PCM provides all the cooling, the electricity requirements for air conditioning are almost negligible. The efficiency increases because the PCM is frozen (energy is stored) when the system operates at its peak efficiency, i.e., while the outdoor temperature is low. The potential value of these savings based on electricity consumption are significant and would add to those from greater local use of PV and from using time-dependent electricity rates to consumers' advantage.

Kedzierski et al. (2018) were able to show that remote PCM storage integrated with a residential ASHP can provide significant energy savings and peak load shifting by generically varying the thermal resistance between the PCM and the refrigerant. In this way, it was demonstrated that the key to maximizing the efficiency of the PCM-TES ASHP

was to minimize the thermal resistance between the PCM material and the refrigerant and the indoor air. It follows that the performance of TES with PCM can be dramatically improved by using direct-contact heat transfer. Direct-contact heat transfer with the PCM eliminates the heat transfer resistance associated with tube walls that typically separate the PCM from the heat transfer fluid. A direct-contact heat exchanger (DCHEX) involves a heat transfer fluid flowing through and in direct contact with an immiscible solid-liquid PCM (SL-PCM). The enhanced heat transfer facilitates and significantly improves the charging/discharging process due to reduced thermal resistances. The improved heat transfer efficiency also allows the use of SL-PCMs that have relatively low thermal conductivity but high latent heat, which improves the energy storage density. In addition, the size and weight of a DCHEX is appreciably smaller than that of a conventional "indirect" heat exchanger due to the elimination of structures like tubes and fins, which also has the additional benefit of reduced capital, material and manufacturing costs. Because of the high energy storage density and the high heat transfer efficiency, along with the significant size and weight savings, PCM-DCHEX can facilitate light, compact, and high-performance thermal energy storage systems.

Despite the benefits associated with PCM-DCHEX, many challenges remain due to the lack of research in this area. Two main areas of interest are direct-contact heat exchange between a PCM and a single-phase fluid and between a PCM and a fluid changing phase. A major concern raised in early studies was whether the freezing PCM would block the flow of the heat transfer fluid and cause equipment failure. Even though the heat transfer fluid can flow through the channels, it may suffer a considerable pressure drop depending on the size of the channel and how the porous structure is formed. The evolution of the path and cross-sectional flow area of passages through a freezing PCM is not well understood and requires further investigation. The existing literature mainly focuses on observations of the multiphase flow pattern and preliminary thermal storage performance measurements, leaving knowledge of the temporal melting/solidification process of a PCM-DCHEX unknown. The effects of flow rate, heat transfer fluid flow pattern and thermodynamic condition (single phase or two phase), nozzle pitch and configuration, and many other factors are still unclear.

Although the structure of PCM-DCHEX is simpler, the heat transfer and fluid flow are more complex, and a temporal pressure drop prediction is not possible. Consequently, this work provides a preliminary design of a direct-contact PCM-TES DCHEX for the NZERTF air-conditioner based on heat transfer and not pressure drop, in two papers (Part 1 and Part 2). Part 1 describes the observation of the direct-contact flow and heat exchange between the PCM and the refrigerant and the selection of the PCM. Part 2 provides the sizing design of the DCHEX, which includes the hole size and placement for the refrigerant orifice place and the height of the PCM column.

2. PCM SELECTION

The present design is complicated by the need to have a PCM material with a very low vapor pressure, phase change at roughly 285 K, and which must be immiscible with the refrigerant. Jankowski and McCluskey (2014) provide an extensive database for thermal energy storage PCMs, including the sugar alcohol glycerol. The database includes material properties such as latent heat, density, melting temperature, specific heat, and thermal conductivity. The study does not provide physical chemistry information that could be used to estimate a PCM's miscibility with a particular fluid. Consequently, the search for a PCM that is immiscible with refrigerant is innately difficult, limited, and largely left to intuition. Refrigerants are generally nonpolar. Consequently, the search should include polar PCMs or those that behave like a polar molecule in hopes that it will not mix with a refrigerant. In addition, thermodynamic properties are primarily determined by the vapor state. Logically, if the PCM has a sufficiently low vapor pressure, its presence in the refrigerant vapor will be negligible, causing the refrigerant to behave as if the PCM wasn't present. In short, the search should begin for readily available PCMs with very low vapor pressures. Glycerol satisfies both of these conditions and it is relatively inexpensive. Glycerol mixes well with water so it acts like it is polar. Its vapor pressure is 0.003 mmHg (0.00006 psia) at 50°C (Jankowski and McCluskey (2014)), which is less than the vapor pressure of many oils.

Glycerol's melting temperature is 291.05 K (Jankowski and McCluskey, 2014), which is approximately 6 K greater than the desired melting temperature for air-conditioning applications. However, because glycerol is a sugar alcohol, it is likely to mix with other sugar alcohols that are used as PCMs to lower the melting temperature. The latent heat of melting of glycerol is 198.7 kJ/kg (Jankowski and McCluskey, 2014), which is relatively large, thus, reducing the required mass for residential air-conditioning.

Two other PCM candidates that are likely to be immiscible with refrigerant due to their low vapor pressures and polarity are octanoic and oleic acid. These are both fatty acids. Octanoic acid melts at 289.25 K with a molar heat of

fusion of 148.6 kJ/kg (Hussain and Kalaiselvam, 2019). It has a vapor pressure of 0.25 Pa at 298 K (Cappa et al., 2008). Oleic acid melts at 278.55 K with a heat of fusion of 20.8 kJ/mol[1] (Inoue et al., 2004) and has a vapor pressure of 1.9×10^{-6} Pa at 298 K (Cappa et al., 2008). Hussain and Kalaiselvam (2019) have studied nanoencapsulated oleic acid PCM with nanoparticles for building thermal energy storage applications. Table 1 provides selected fluid properties for oleic and octanoic, which were taken from Valeri and Meirelles (1997), Cappa et al. (2008), Hussain and Kalaiselvam (2019), and Nunes et al. (2019).

Table 1 Selected fluid properties of PCMs and R410A[2] at or near T_v or T_m

Fluid	$T_{v\ OR}$ T_m (K)	P_v (kPa)	Pr_v (-)	k_l ($mWm^{-1}K^{-1}$)	μ_l ($\mu kg \cdot m^{-1} \cdot s^{-1}$)	σ ($N \cdot m^{-1}$)	ρ_l ($kg\ m^{-3}$)	ρ_v ($kg\ m^{-3}$)	i_{fg} OR i_{fg} ($kJ\ kg^{-1}$)	c_{pl} ($kJkg^{-1}K^{-1}$)
Oleic acid	278.55	1.9×10^{-6}	219.0	224.0	24000.0	0.033	892.0	(-)	140.20	2.046
Octanoic acid	289.25	2.5×10^{-4}	105.4	147.0	7500.0	0.039	910.0	(-)	148.59	2.0656
R410A	282.0	1048.4	2.3	98.2	144.81	0.007	1133.3	40.45	210.04	1.5710

2.1 Benchtop Miscibility Tests

Glycerol was mixed with R123 in a glass jar and the mixture was observed to be completely immiscible from room temperature to approximately 260 K. The same tests were done with an octanoic acid and R123 and the mixture was found to be miscible from room temperature to approximately 260 K. It was hypothesized that the miscibility of R123 with the octanoic acid was due to the chlorine atom in R123.

Figure 1 shows a schematic of the test vessel that was constructed to observe a mixture of octanoic acid with R134a, which does not contain chlorine. The test vessel was designed to observe high pressure fluids up to 20 atm. The site glass window was a commercial site glass used for air-conditioning and refrigeration purposes. Copper tubing was used to connect the site glass to a refrigeration valve and to cap the lower end of the site glass. Tests with octanoic

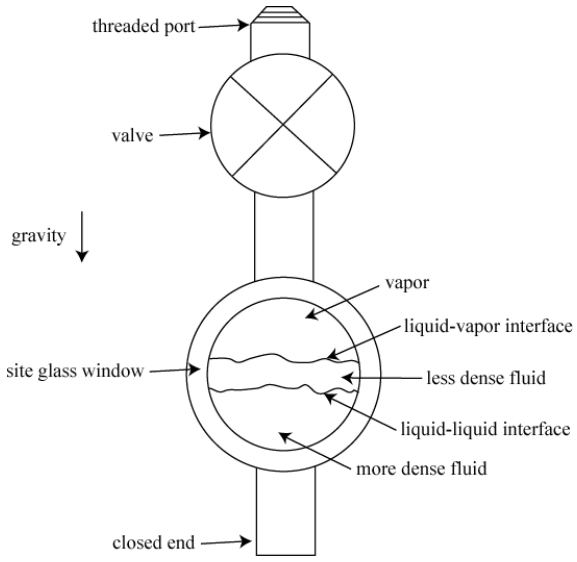

Figure 1 Schematic of pressure vessel to observe miscibility

[1] 73.63 kJ kg^{-1}

[2] Obtained from REFPROP 10.0 while using the default equations (Lemmon et al., 2018)

acid and R134a using the test vessel showed that the mixture was immiscible at room temperature. Likewise, R134a and glycerol were observed to be immiscible.

Because of glycerol's immiscibility with both R123 and R134a, and its lower cost, it was chosen over octanoic acid for the flow observation tests (Part 1). Because the melting temperature of octanoic acid was closer to the air-conditioning application than that of oleic acid, octanoic acid was chosen as the PCM for the DCHEX design (Part 2).

3. EXPERIMENTAL APPARATUS

Figure 2 shows a sketch and picture of the experimental apparatus that was used to observe the direct-contact, two-phase flow between the refrigerant and the PCM. The experimental test facility consisted of a single refrigerant loop with heat exchangers, a magnetically coupled gear pump, and a visualization section. The refrigerant flow rate, pressure, and liquid subcooling were fixed at the inlet to the test section. The chilled water flow to a brazed plate heat exchanger was used to condense refrigerant vapor and to control the amount of refrigerant subcooling delivered to the pump via a second brazed plated subcooler. Subcooled refrigerant flow was diverted to the observation test section from the pump. A combination of refrigerant bypass valve and inverter frequency variation was used to set the flowrate of subcooled refrigerant to the test section. Six instream, sheathed thermocouples in the test section were used to measure the PCM temperature. The temperature of the refrigerant entering the test section was measured with a thermocouple attached to the outside of the inlet refrigerant tube and covered with insulation. The refrigerant vapor exiting the test section was delivered to a brazed plate evaporator, and mixed with the subcooled refrigerant flow that bypassed the test section. The evaporator, the condenser, and the subcooler were used in concert to maintain and establish a constant pressure and to allow for subcooling. The refrigerant pressure at the exit of the test section was monitored with a dial pressure gauge.

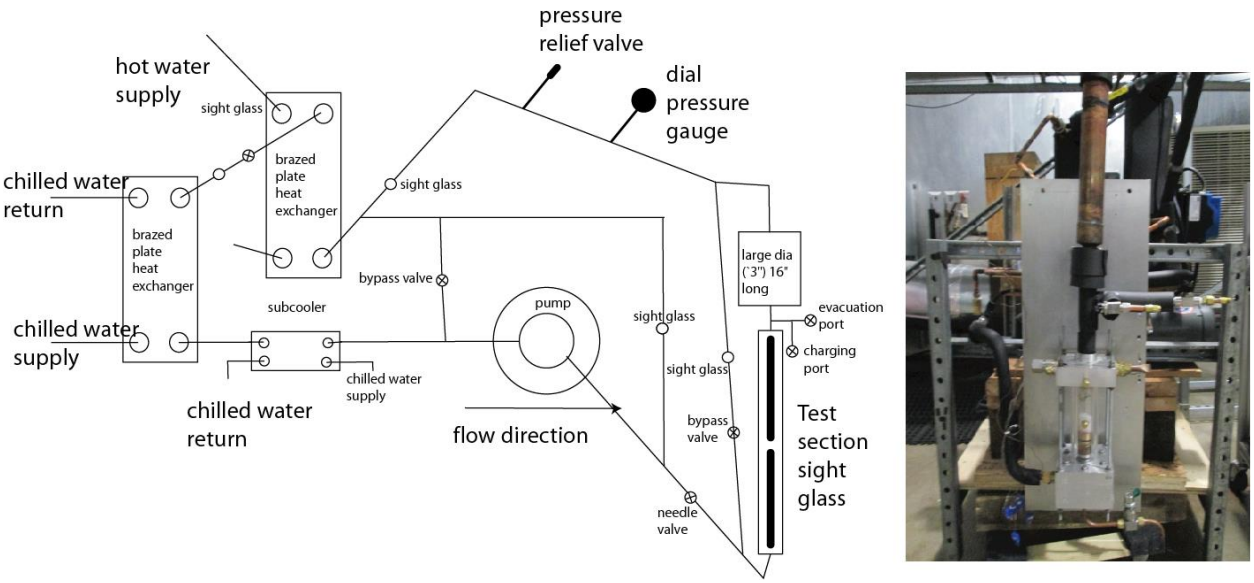

Figure 2 Schematic and photo of PCM/refrigerant flow observation test apparatus

The test section, shown in Fig. 3, consisted of concentric, vertical tubes approximately 185 mm in length. The inner tube or column was made of quartz and had an inner and outer diameter of approximately 28.3 mm and 34.5 mm, respectively. The inner tube contained the PCM and PTFE Raschig ring packing. Raschig rings are short cylinders generally having lengths equal to their diameters (McCabe and Smith, 1976). The Raschig rings where approximately 3 mm in diameter and length and filled approximately one third of the column height. The packing was held in place at the bottom of the column by a liquid refrigerant distribution plate with twenty 1 mm diameter orifice holes. The packing was used to promote refrigerant flow through the PCM as it froze. A plexiglass tube surrounded and was concentric with the inner quartz tube for safety. The space between the plexiglass tube and the quartz tube could be evacuated in order to reduce heat transfer to the surroundings and to prevent condensation of moist air onto the quartz tube, which would have increased

heat transfer and reduced visibility. A digital video camera was used to record the direct contact heat exchange that occurred between the PCM and the refrigerant in the quartz tube.

A fixed test pressure was maintained by balancing the refrigerant duty between the subcooler, the test section, the preheater and the condensers. A magnetically coupled gear pump delivered the test refrigerant to the entrance of the test section as

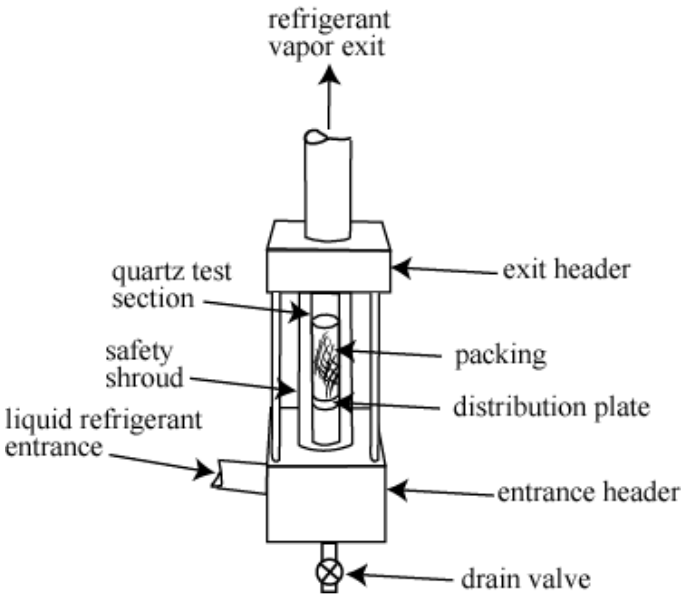

Figure 3 Schematic of PCM/refrigerant test section

subcooled liquid. Further subcooling was achieved by packing the outside of the test section inlet with dry ice. This was done to reach temperatures near 260 K. The inlet temperature of the water loop was held constant for each test with a water-chilled heat exchanger where the fluid flow was varied to control the heat duty. The refrigerant flow rate was controlled by varying the pump speed using frequency inverters. The flow rate was set to evaporate all the refrigerant before it exited the PCM in the observation test section.

Figure 2 shows the location of the test section in the test rig. The inner tube of the test section was constructed of quartz and was sealed with a cylindrical insert with double o-rings at both ends. Five stainless steel sheathed thermocouples passed through the cylindrical insert and into the test section packing. This construction permitted the measurement of the PCM and the packing temperature at five different positions along the vertical test section. In addition, thermocouples were attached to the outside surface the refrigerant tube at the inlet and outlet of the test section. The test apparatus was wrapped with approximately 2 cm of foam insulation to minimize heat transfer between the test fluids and the ambient.

4. FLOW OBSERVATIONS

Figure 4 shows a sketch of the primary flow patterns that were observed for evaporating R134a rising through glycerol in the quartz column of the above test apparatus. The bubbles shown on the right side of the column contain liquid R134a, which evaporates as the bubble rises. The bubbles leave tails that trail below the bubbles and elongate as they rise due to the highly viscous nature of glycerol. For sufficiently numerous bubbles, the elongated tails of bubbles agglomerate into a vapor rivulet that forms a path for smaller bubbles. As the glycerol becomes more viscous due to cooling, the rivulets remain established and permit the flow of bubbles containing liquid to rise through it. Although the glycerol never completely froze, the path of the rivulets remained fixed once the glycerol reached approximately 260 K. Consequently, the paths are likely to remain open at the freezing point because the fluid contracts upon freezing.

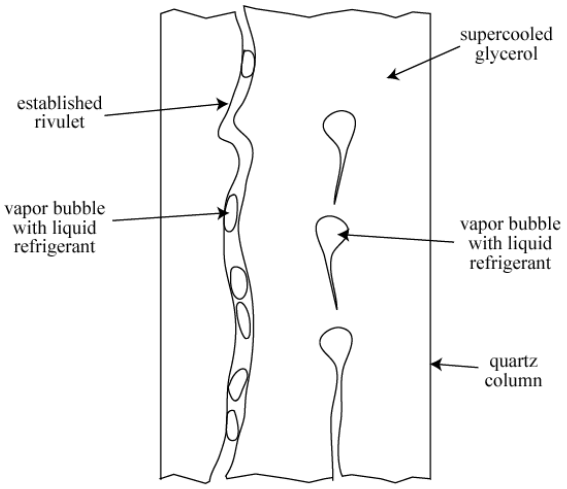

Figure 4 Primary flow patterns for evaporating R134a rising through glycerol

5. GLYCEROL SUPERCOOLING

One problem with glycerol as a PCM that was not immediately realized by the authors is that glycerol significantly supercools before it freezes. In fact, glycerol will not freeze unless it is brought below 190 K and then heated to 238.7 K where it will freeze. The point at which glycerol freezes depends on the warming rate (Sou, 2011). Figure 5 plots differential scanning calorimetry (DSC) thermogram data from Sou (2011) that demonstrates the melting and freezing characteristics of glycerol at 0.5 mK/s. In general, glycerol does not crystallize (i.e., freeze) when cooled to its melting point (292 K) under normal conditions, due to the strong hydrogen bond associated with the hydroxyl groups. Instead, it remains as a supercooled, highly viscous liquid until it turns into an amorphous state at the glass

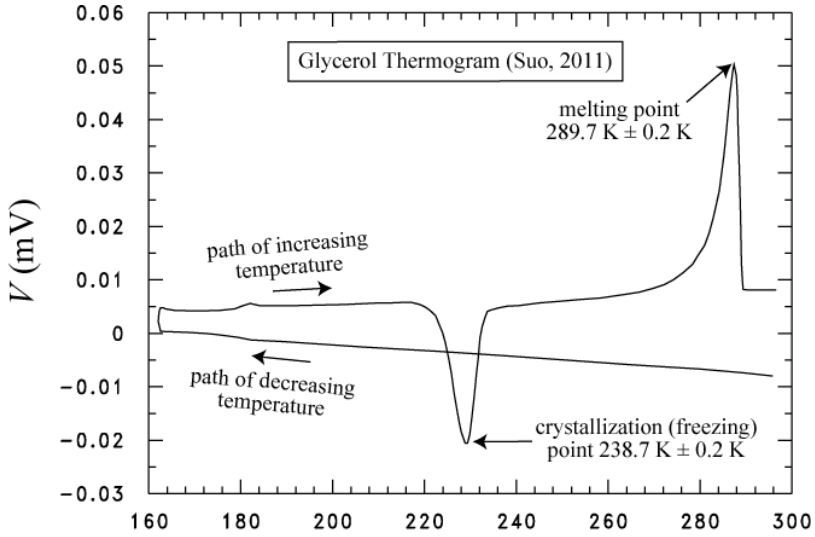

Figure 5 Glycerol thermogram (Sou, 2011)

transition point temperature (~160 K). The crystallization of glycerol occurs when warming up the glassy glycerol and at approximately 210 K to 260 K, depending on the heating rate.

The authors tried to mitigate the supercooling and freeze the glycerol by adding zinc oxide nanoparticles without success. In fact, the supercooling of glycerol has been an unsolved problem for over a century, and glycerol has been used as an effective antifreeze additive due to the supercooling effect. The existing methods that can crystallize glycerol when cooling are based on seeding the liquid glycerol with premade glycerol crystals (Gibson and Glauque (1923) and Hass and Patterson (1941)). However, this method cannot be applied to thermal energy storage because the crystals need to be replenished between each freezing and thawing cycle. In addition, the glycerol crystallization process is slow and unstable.

6. CONCLUSIONS

Direct-contact heat exchange can be used to significantly reduce the thermal resistances associated with charging and discharging phase change material (PCM) by eliminating physical barriers that significantly contribute to the heat transfer resistance between the refrigerant and the PCM. High efficiency thermal energy storage (TES) for a residential air-conditioner can be achieved by using direct-contact heat transfer.

A visualization test apparatus was constructed to observe the flow of refrigerant through the PCM. Glycerol was used as the PCM because of its immiscibility with R134a and its relatively low cost. R134a was used as the refrigerant for its significantly lower vapor pressure as compared to R410A, which would keep the operating pressure well below the burst limit of the quartz observation test section. The tests verified that refrigerant continues to flow through the PCM as it freezes without producing a total blockage of flow. These tests can assist in the design of a direct-contact heat exchanger for PCM/refrigerant working fluids. Future work should focus on optimizing the PCM to meet the DCHEX requirements (i.e., low vapor pressure, immiscible with refrigerant at operating temperatures, phase change at approximately 285 K with insignificant supercooling, relatively high latent heat and thermal conductivity) and performing systematic measurements for each property of interest.

NOMENCLATURE

English symbols		**Greek symbols**	
c_p	specific heat (kJ·kg^{-1} K^{-1})	μ	dynamic viscosity (kg·m^{-1}·s^{-1})
i_{fg}	latent heat of vaporization (kJ·kg^{-1})	ρ	density (kg·m^{-3})
i_{fs}	heat of fusion (kJ·kg^{-1})	σ	surface tension (N·m^{-1})
k	thermal conductivity (W·m^{-1}·K^{-1})		
Pr	Prandtl number (-)		
T	temperature (K)		
V	voltage (V)		

Subscripts

l	liquid
m	melting
v	vapor

REFERENCES

ASHRAE. 2015. 2015 ASHRAE Handbook -HVAC Systems and Equipment, Chapter 51, Atlanta, GA, p. 51-1.

Baxter, V.D., and Moyers, J.C. 1985. Field-measured cycling, frosting, and defrosting losses for a high-efficiency air-source heat pump. ASHRAE Trans. Vol. 91:2B. 537-554.

Cappa, C.D., Lovejoy, E.R., Ravishankara, A.R. 2008. Evaporation rates and vapor pressures of the even-numbered C 8-C18 monocarboxylic acids. J. Phys. Chem. A 112, 3959–3964. https://doi.org/10.1021/jp710586m

Fanney, A. H., Payne, V., Ullah, T., Ng, L., Boyd, M., Omar, F., Davis, M., Skye, H., Dougherty, B., Polidoro, B., Healy, W., Pettit, E., 2015. Net-zero and beyond! Design and performance of NIST's net-zero energy residential test facility, Energy and Buildings, 101, 95–109. http://dx.doi.org/10.1016/j.enbuild.2015.05.002

Gibson, G.K., Glauque, W.P. 1923. The third law of thermodynamics. Evidence from the specific heats of glycerol that the entropy of A glass exceeds that of a crystal at the absolute zero, J. Am. Chem. Soc. 45 93–104. doi:10.1021/ja01654a014.

GPSA. 2004. Engineering Data Book, Gas Processors Suppliers Association (GPSA), 12th ed, Tulsa, OK, p. 7-11.

Hass, H.B., Patterson, J.A. 1941. Purification of Glycerol by Crystallization, Ind. Eng. Chem. 33 615–616. doi:10.1021/ie50377a015.

Hussain, S. I., and Kalaiselvam, S. 2019. Nanoencapsulation of oleic acid phase change material with Ag2O nanoparticles-based urea formaldehyde shell for building thermal energy storage, Journal of Thermal Analysis and Calorimetry https://doi.org/10.1007/s10973-019-08732-5(0123456789().,-volV)(0123456789,-().volV)

Inoue, T., Hisatsugu, Y., Suzuki, M., Wang, Z.N., Zheng, L.Q. 2004. Solid-liquid phase behavior of binary fatty acid mixtures: 3. Mixtures of oleic acid with capric acid (decanoic acid) and caprylic acid (octanoic acid). Chem. Phys. Lipids 132, 225–234. https://doi.org/10.1016/j.chemphyslip.2004.07.004

Jankowski, N.R., McCluskey, F.P., 2014. A review of phase change materials for vehicle component thermal buffering. Appl. Energy 113, 1525–1561. https://doi.org/10.1016/j.apenergy.2013.08.026

Kedzierski, M. A., Payne, W. V., and Skye, H. M. 2018. Thermal Energy Storage for the NIST Net-Zero House Heat Pump, NIST Technical Note 2005, U.S. Department of Commerce, Washington, D.C.

Lemmon, E. W., Bell, I. H., Huber, M. L., and McLinden, M. O. 2018. *NIST Standard Reference Database 23 (REFPROP), Version 10*., National Institute of Standards and Technology, Boulder, CO.

McCabe, W. L., and Smith, J. C. 1976. Unit Operations of Chemical Engineering, 3rd ed., McGraw-Hill, pp. 709-710.

Nunes, R.J., Saramago, B., Marrucho, I.M. 2019. Surface Tension of dl -Menthol:Octanoic Acid Eutectic Mixtures. J. Chem. Eng. Data 64, 4915–4923. https://doi.org/10.1021/acs.jced.9b00424

Payne, W. V. 2018. Private Communications. The National Institute of Standards and Technology, U.S. Department of Commerce, Washington, D.C.

Sou, K. 2011. High-resolution Calorimetry on Thermal Behavior of Glycerol (Evolution of Personal Desk Lab (PDL) System to a Research Use). Ph.D. Thesis, Chiba University, Chiba, Japan.

Valeri, D., Meirelles, A.J.A. 1997. Viscosities of fatty acids, triglycerides, and their binary mixtures. JAOCS, J. Am. Oil Chem. Soc. 74, 1221–1226. https://doi.org/10.1007/s11746-997-0048-6

ACKNOWLEDGEMENT

This work was funded by Exploratory Research Project of the National Institute of Standards and Technology (NIST). Thanks go to Dr. Riccardo Brignoli and to Dr. W. Vance Payne of NIST for their constructive criticism of the draft manuscript.